Spectral characterization of bulk and nanostructured aluminum nitride

Baiba Berzina,[a] Laima Trinkler,[a] Darja Jakimovica,[a] Valdis Korsaks,[a] Janis Grabis,[b] Ints Steins,[b] Eriks Palcevskis,[b] Stefano Bellucci,[c] Li-Chyong Chen,[d] Surojit Chattopadhyay,[d] and Kuei-Hsien Chen[d]

[a] University of Latvia, Institute of Solid State Physics, Kengaraga 8, Riga LV-1063, Latvia
baiber@latnet.lv

[b] Technical University of Riga, Institute of Inorganic Chemistry, Azenes 14, Riga, Latvia

[c] INFN-Laboratori Nazionali di Frascati, Via Enrico Fermi 40, I-00044 Frascati, Italy

[d] Taiwan National University, Center for Condensed Material Sciences, Taiwan

Abstract. Spectral characteristics including photoluminescence (PL) spectra and its excitation spectra for different AlN materials (AlN ceramics, macro size powder and nanostructured forms such as nanopowder, nanorods and nanotips) were investigated at room temperature. Besides the well known UV-blue (around 400 nm) and red (600 nm) luminescence, the 480 nm band was also observed as an asymmetric long-wavelength shoulder of the UV-blue PL band. This band can be related to the luminescence of some kind of surface defects, probably also including the oxygen-related defects. The mechanisms of recombination luminescence and excitation of the UV-blue luminescence caused by the oxygen-related defects were investigated. It was found that the same PL band is characteristic for different AlN materials mentioned above; however, in the nanostructured materials (nanorods, nanotips and nanopowder) the intensity of UV-blue PL is remarkable lower than in the bulk material (ceramics). In the case of nanostructured AlN materials, excitation of the oxygen-related defect is mainly realized through the energy transfer from the host material (electron/hole or exciton processes) to the defects and this mechanism prevails over the mechanism of direct defect excitation.

Keywords: Aluminum nitride, ceramics, norods, nanopowder, nanotips, photoluminescence.

1 INTRODUCTION AND PROBLEM

Aluminum nitride (AlN) is one of prospective wide band-gap materials (E_g = 6.2 eV [1,2]) possessing a number of extraordinary features such as high melting point (~2200 ^{0}C), good thermal and chemical stability, high resistivity and thermal conductivity (~275 $W \cdot m^{-1} \cdot K^{-1}$) providing its application in devices, which also could work in extreme environmental conditions. In optoelectronics AlN is used as a dielectric layer in optical storage media and a heat conductor in devices where high thermal conductivity is essential. Besides, it is found that AlN itself is a good storage material for UV light irradiation and its application in this field seems promising [3-10]. Recently exciton luminescence in the spectral range around 200 nm was observed for AlN single crystals [11, 12] and nanotips [13] revealing its lasing material behaviour.

Optical properties of AlN largely depend not only on its structure but also on defect type and amount in the material. These defects usually form their energy levels within the band gap and their spectral characteristics fall into the UV or visible spectral range. Thus the luminescence-based spectral investigation of material is convenient and could give valid information about the processes occurring in the crystalline lattice of AlN caused by

Received 23 Jul 2009; accepted 24 Nov 2009; published 3 Dec 2009 [CCC: 19342608/2009/$25.00]

irradiation with UV light or ionizing radiation, as well as allows reveal defect structure responsible for luminescence.

AlN is also a good medium for studying of the effect of dimensionality on optical properties when the material size diminishes from bulk to nanoscale formations. Presently different forms of nanostructured AlN are available including nanopowders [14], nanotubes [15-22], nanotipes, nanorods [23] etc. Spectral studies of these materials are actual and currently going on in many laboratories of the world.

Luminescence processes in AlN can be related to the host material luminescence including electron-hole recombination and exciton luminescence as well as to the defect-induced luminescence. The exciton luminescence has been observed comparatively recently. It was found that in the cathodoluminescence (CL) spectra of AlN thin layers the 6.04 eV and 6.01 eV bands appear related to the free exciton and localized exciton emission, correspondingly [11]. The same exciton luminescence is observed in PL spectra of AlN single crystals [12] and CL spectra of AlN nanotips [13]. The exciton luminescence is better observed at low temperatures (region of liquid helium temperature (LHeT) and above), whereas at room temperature (RT) it is partly suppressed by the defect luminescence.

There is a large variety of defects probably responsible for luminescence in AlN. The host material defects such as vacancies of Al and N ions (v_{Al} and v_N), their antisites (Al_N; N_{Al}), interstitials etc. are some of the relevant defect types. Besides, there can be native defects like an oxygen ion substituting for a nitrogen (O_N) always present in the crystalline lattice of AlN as well as impurity ions (C, Zn, Mg etc.) specially introduced in the crystalline lattice. All these defects form their energy levels within the band gap of AlN. Some of them could be related to donor centers (with energy levels close below the conduction band bottom) such as v_N, N_{Al}, Al_N, whereas others – to acceptor centers (with energy levels close above the valence band top) such as v_{Al}, v_{Al}-O_N, C_N, Mg_{Al} etc. These defects could form separate luminescence centers or participate in recombination processes resulting in emission located within a wide spectral region. Spectral characterization of the defect luminescence has begun a few decades ago. There are two main luminescence bands located within the UV-visible spectral range observed for the bulk AlN and caused by native defects. The UV-blue band is situated around 3.1 eV (400 nm) and its position varies from 3.54 eV (350 nm) up to 2.95 eV (420 nm) for samples of different origin [27]. The oxygen-related defect structure and recombination nature of the UV-blue luminescence was proposed [24-28]. The other luminescence band is located around 2.07 eV (600 nm) and its nature is not clear yet. Luminescence processes within the spectral range from 250 nm up to 700 nm were studied by the authors of this paper for AlN bulk material [29-31], AlN nanotips and nanorods [32, 33], AlN nanopowder [14] and AlN nanotubes [34].

The present work is devoted to the study of luminescence properties of AlN observed within the UV and visible spectral range caused by native defects in order to reveal luminescence mechanisms and defect types involved in this process as well as to compare the results obtained for the bulk AlN and its nanostructured forms.

2 MATERIALS AND INVESTIGATION METHODS

2.1 Materials

Bulk material. The bulk material used for the present studies is AlN ceramics prepared using a plasma synthesis method and Y_2O_3 additive in the Institute of Inorganic Chemistry, Riga Technical University, Latvia [29]. It is grey coloured solid material consisting of the AlN polycrystalline grains with diameter of ~4 mkm and Y_2O_3 additive filling the interspace between these grains. The additive was used as a sintering aid. The 1 mm thin plates of this ceramics were used as samples for spectral measurements. The samples with different oxygen concentration in AlN grains were produced by varying the sintering temperature and time as

well as concentration of the Y_2O_3 additive. In order to determine the potential influence of Y_2O_3 additive on AlN spectral properties another type of ceramics made in Japan without Y_2O_3 additive was also used. The spectra observed for these two materials within the spectral range between 250 nm and 700 nm were similar and thereby a visible influence of Y_2O_3 on spectral characteristics of the material was not found. The raw material of the AlN ceramics made in Latvia – the AlN macrosize powder was also studied.

Nanostructured AlN powder. The AlN nanostructured powder is synthesized in the Institute of Inorganic Chemistry, Riga Technical University, Latvia [35]. It was found that AlN nano-particles have a shape of hexagonal plates and according to TEM data the size of these particles is within a range of 20–60 nm.

AlN nanotips and nanorods. These nanostructured materials are produced in Taiwan National University, Taiwan [23]. The nanotips form a cone with approximate diameters 10 nm at the top and 100 nm at the base. Their lengths are around 2000 nm. The diameters of nanorods are approximately 20 nm and greater.

2.2 Experimental

Photoluminescence (PL) spectra within the spectral range 250 - 700 nm and its excitation (PLE) spectra (210 – 400 nm) were studied at room temperature (RT). A conventional self-made setup was used consisting of two monochromators for filtering the excitation light and luminescence light, a deuterium lamp (400 W) as UV light source, a sample holder and the luminescence recording system based on photoelectron multiplier. All the corrections necessary for the PL and PLE spectra due to the equipment characteristics have been done.

3 PHOTOLUMINESCENCE AND ITS EXCITATION SPECTRA

Photoluminescence spectra and its excitation spectra of AlN ceramics, AlN powder and AlN nanostructured forms: nanopowder, nanotips and nanorods were studied at room temperature.

3.1 Spectra of AlN ceramics

The PL spectra for AlN ceramics (produced in Latvia) at RT are shown in Fig.1. These spectra are measured under the same experimental conditions using three different wavelengths of exciting light related to one and the same constant number of exciting light quanta thus demonstrating the relative yield of PL observed under different excitations. The first PL spectrum (1) is measured under 200 nm (6.2 eV) excitation corresponding to the low energy part of the fundamental absorption edge of AlN resulting in generation of an electron/hole pair or an exciton. The next two spectra (2) and (3) are measured exciting the sample with light from two local defect-induced absorption bands (seen in Fig. 2) at 245 nm (5.06 eV) and 285 nm (4.35 eV). It is seen that intensity of the complex luminescence spectra decreases when wavelength of the exciting light is changed from 200 nm to 245 nm and 285 nm.

The shapes of all three complex luminescence spectra are similar (Fig. 1). Each spectrum consists of two broad bands located in the UV-visible spectral range. One of them is located around 600 nm (2.07 eV) (the red band). The other part of the PL spectra forms a broad asymmetric band within the UV-blue spectral region and it seems also to be complex consisting of at least two sub-bands located around 400 nm (3.1 eV) and 480 nm (2.58 eV) although the first of them is predominant. These bands are better pronounced at 200 nm excitation (Fig. 1, curve 1). Presence of these two luminescence sub-bands is confirmed by the PLE spectra shown in Fig. 2 where it is seen that each PL sub-band is related to its own local excitation band: excitation of the 400 nm PL is located at 245 nm, whereas excitation of

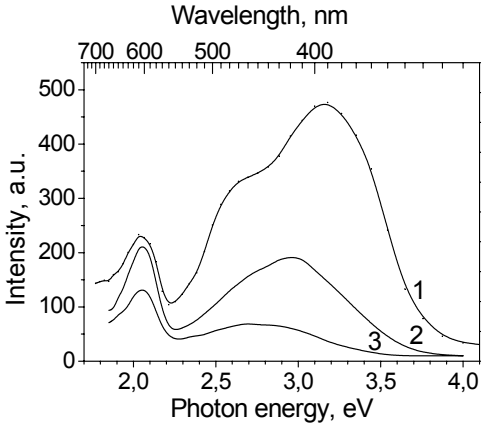

Fig. 1. AlN ceramics. PL spectra at RT using the following excitations: 1 – 200 nm; 2 – 245 nm; 3 – 285 nm. All three PL spectra are related to one and the same constant number of exciting light quanta.

the 480 nm PL – at the 285 nm. Besides, all of the PL sub-bands can be excited also at 200 nm through exciton or electron/hole processes.

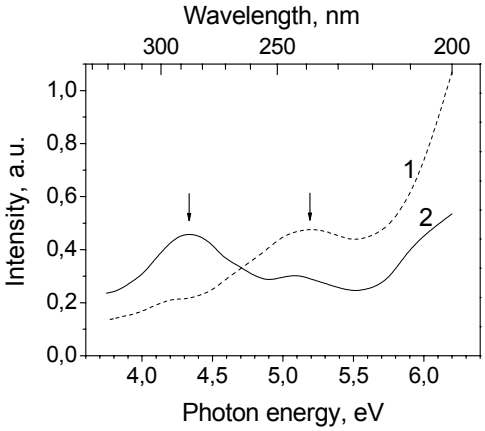

Fig. 2. AlN ceramics. PLE spectra at RT for the following narrow (~20 nm) spectral intervals of PL: dash line around 400 nm (1); solid line – around 480 nm (2). The arrows show band maxima.

It was found that intensity of the 400 nm PL depends on duration of continuous irradiation within its direct excitation band at 245 nm (Fig. 3A). At the beginning of irradiation the PL intensity is low then during irradiation its intensity gradually increases and reaches the saturation after approximately 30 min. The afterglow of PL after ceasing of exciting irradiation is also observed (Fig. 3B). It was found that the spectral position of the UV-blue PL band is also dependent on duration of exposition to 245 nm light and the "red shift" of PL spectra with increase of exposition time is observed. Figure 4 shows three PL spectra. One of them (1) is measured when exposition time to 245 nm exciting light is short – only 2 s. The second one (2) is measured when exposition time is 30 min and the saturation of PL intensity

is reached, whereas the third one is the spectrum of luminescence afterglow. All three spectra are normalized for maximum intensity.

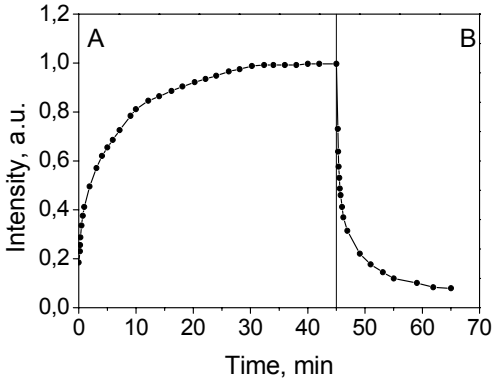

Fig. 3. AlN ceramics. A – rise of UV-blue PL intensity under continuous excitation with 245 nm light. B – luminescence afterglow – decay of PL intensity after ceasing of excitation.

It is seen that the shape of the complex PL spectra (245 nm excitation) is sensitive to the oxygen concentration in the crystalline lattice of AlN (Fig. 5). Increase of the oxygen concentration (from D to A) results in the shift of the UV-blue PL band towards the low energy side (the red shift). (Unfortunately, the present experiment did not allow accurate evaluation of oxygen concentration). This fact is in a good agreement with that reported in [27, 28]. In the same time, the ratio of the intensities of blue and red luminescence bands is different for various samples.

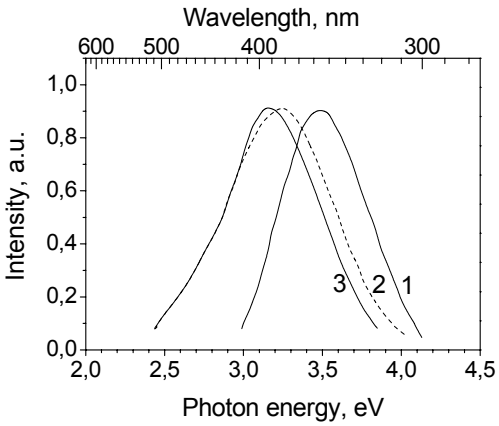

Fig. 4. AlN ceramics. The UV-blue luminescence spectra measured under the following experimental conditions: 1 – sample is excited with short (2 s) pulses of 245 nm light; 2 – continuous excitation with 245 nm light after 30 min exposition (shown in Fig. 3 A); 3 – a spectrum of the luminescence afterglow.

The excitation spectra of the red luminescence at 600 nm are shown in Fig. 6. Besides the fundamental absorption edge at 200 nm two excitation bands at 255 nm (4.86 eV) and 400 nm

(3.1 eV) are observed (see the arrows at Fig. 6, curve 1). The first PLE band at 255 nm partly overlaps with the ~245 nm PLE band for UV-blue PL (see the arrow at Fig.6, curve 2). The second excitation band of the red luminescence is located at 400 nm (3,1 eV) and exactly overlaps with the broad UV-blue PL band resulting in its reabsorption and transformation into the red PL.

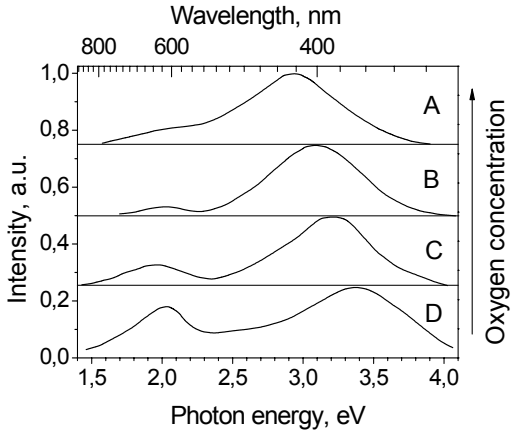

Fig. 5. AlN ceramics. PL spectra measured at 245 nm excitation for the samples with different oxygen concentration in AlN grains. This concentration is growing in from D to A.

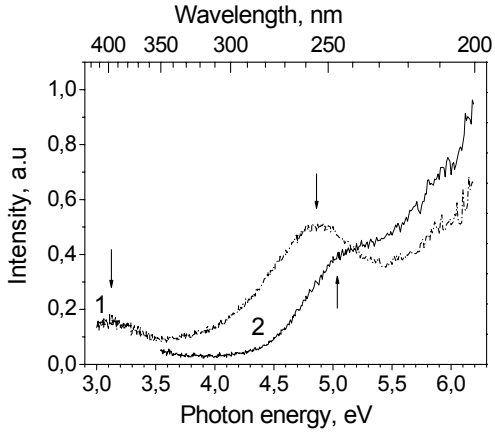

Fig. 6. AlN ceramics. 1 - excitation spectrum of 600 nm PL band; 2 – excitation spectrum of 400 nm PL band. The arrows show positions of the bands maxima.

3.2 Spectra of AlN macrosize powder and nanostructured powder

PL spectra of macrosize AlN powder and nanosize powder are shown in Fig. 7 and Fig. 8, respectively. For these materials two PL spectra are measured under excitations 242 nm (curve 1) and 283 nm (curve 2). According to the results above these excitations are directly

related to the 400 nm and 480 nm PL bands, correspondingly (see Fig. 2). It is seen that in the case of the AlN powders the 480 nm PL band becomes predominant while the 400 nm PL band is hardly detectable (Figs. 7 and 8). In the case of AlN powders the red PL band observed for AlN ceramics (Fig.1) has not been seen.

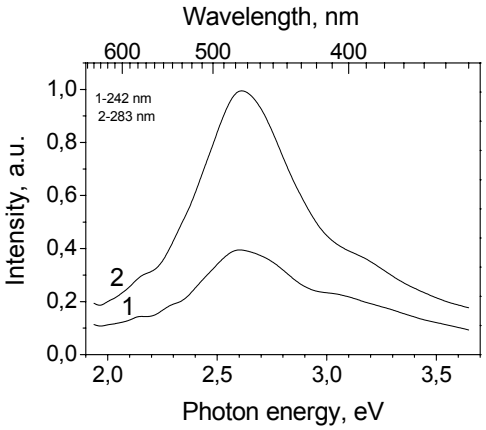

Fig. 7. AlN powder – a raw material of AlN ceramics. The PL spectra at the following excitations: 1 – 245 nm; 2 – 283 nm.

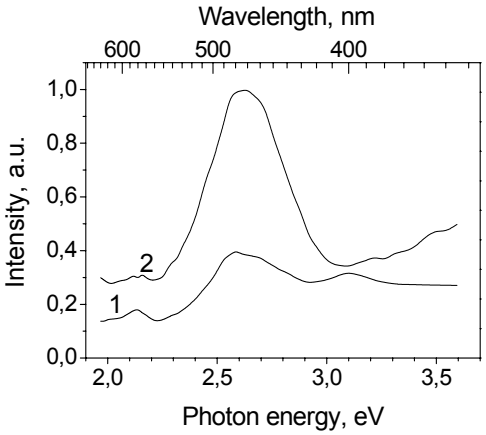

Fig.8. AlN nanostructured powder. PL spectra at the following excitations: 1 - 245 nm; 2 – 283 nm.

3.3 Spectra of AlN nanorods and nanotips

PL spectra of AlN nanorods and nanotips are shown in Fig. 9, curves 2 and 3, respectively, together with the PL spectrum of AlN ceramics (curve 1). All three spectra are measured under the same experimental conditions at 200 nm excitation. All these results are related to equal number of exciting light quanta for each measurement, thus demonstrating luminescence yield depending on material type. It is seen that efficiency (intensity) of luminescence for nanorods and nanotips is considerably lower than that for the AlN ceramics. The same spectra are shown in Fig. 10 after normalization for maximum intensity. It is seen

that the structure of complex PL spectra for all three samples is similar. In the case of nanorods and nanotips the 400 nm PL band is predominant and intensity of the 480 nm PL is comparatively low, besides the 600 nm band also appears. These spectral features differ from those observed for AlN nanopowder (Fig. 8).

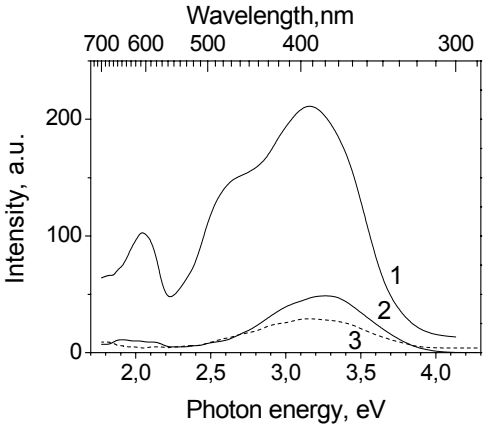

Fig. 9. PL spectra for: 1 – AlN ceramics, 2 – AlN nanorods, and 3 - AlN nanotips. All spectra are measured under the same experimental conditions using 200 nm exciting light.

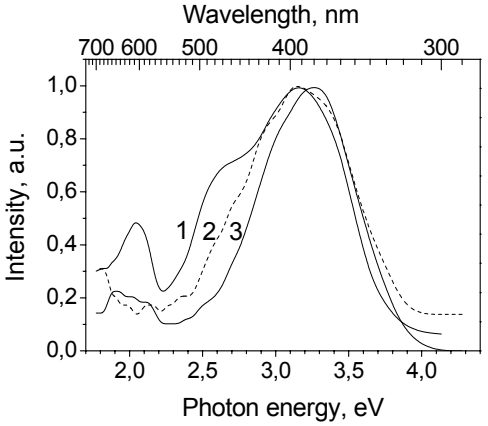

Fig. 10. The same PL spectra as in Fig. 9 but normalized (200 nm excitation). 1 – AlN ceramics, 2 – AlN nanorods, and 3 - AlN nanotips

Excitation spectrum of AlN nanorods for blue luminescence is shown in Fig. 11. It is seen that the PL is mainly excited within the fundamental/exciton absorption band but the defect related absorption/excitation band is not clearly pronounced. The PLE spectrum of AlN nanotips is very similar to that of the nanorods.

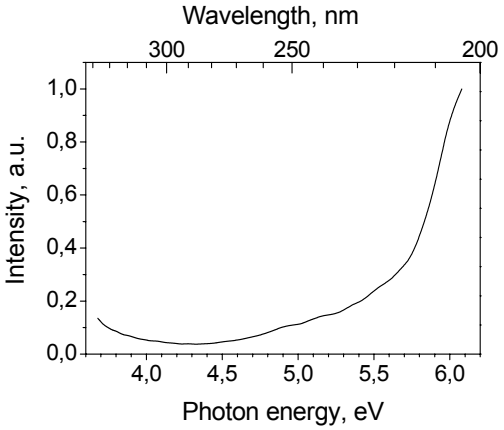

Fig. 11. AlN nanorods. PLE spectrum of 380 nm luminescence.

4 DISCUSSION

Analysis of the PL and its excitation spectra observed together with those from literature data can give insight into type and structure of defects providing luminescence as well as allows reveal the processes and luminescence mechanisms responsible for the PL bands observed. Moreover, various AlN structures investigated allow evaluation of the dimension effect on luminescence processes when material transforms from the bulk AlN to its nanostructured forms.

4.1 Photoluminescence mechanisms and defects involved

Three different PL bands observed in AlN within the UV-visible spectral range are discussed in this paper. The results above confirm that intensity and ratio of these bands strongly depend on excitation type and material structure. Analysis of the origin of these luminescence bands follows.

4.1.1 UV-blue luminescence

The UV-blue PL band around 400 nm is the most investigated among the PL bands observed for AlN especially for its bulk form (ceramics). Its recombination character caused by the oxygen-related defects have been discussed initially by Youngman, Harris, Slack et al ([26, 27] and references therein) and also in our previous works [29-31]. The recombination character of the UV-blue PL is confirmed by the following results above: *i)* time-dependent slow increase of PL intensity under 245 nm continuous excitation and its slow decay after ceasing the exciting light (Fig. 3), *ii)* this band appears in luminescence afterglow spectra (Fig. 4, curve 3). Besides, it is known that the UV-blue band predominates in spectra of optically-stimulated luminescence (OSL) and thermo-stimulated luminescence (TL) [3-10]. It means that this luminescence is not caused by the intrinsic processes occurring inside of a single excited defect but that at least two types of defects form the luminescence center responsible for the UV-blue emission.

It was previously proposed by Slack, Youngman and Harris [24-28] that the oxygen-related defects are responsible for the UV-blue PL in AlN. Recently the ODMR studies of AlN ceramics have been performed and a good agreement of the results obtained for the UV-blue luminescence with the oxygen-related defect structure causing this luminescence was demonstrated [36]. According to these results one of defects forming the luminescence center

(a hole part) is an Al vacancy (v_{Al}) together with a close oxygen substituting for nitrogen (O_N) resulting in (v_{Al}-O_N) pair formation, but the other one (an electron part) is another closely situated oxygen (O_N).

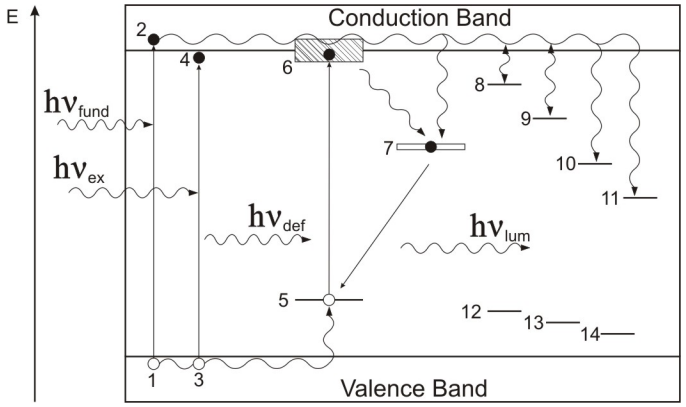

Fig. 12. Energy level scheme of AlN crystalline lattice illustrating the luminescence processes. The details are explained in the text.

The concept of the luminescence center containing oxygen–related defects together with the spectral properties of the UV-blue luminescence allows proposing of an energy level scheme illustrating the recombination luminescence process and luminescence mechanism (Fig. 12). The first attempt to construct this scheme was done in one of our previous works [31]. According to the scheme depicted on Fig.12 the (v_{Al}-O_N) pair forms its energy level within the band gap above the valence band (level 5). Irradiation of AlN with 245 nm light from the absorption band of this defect pair (hv_{def}) results in its excitation (level 6). It seems that this excited state is situated close below the bottom of the conduction band or may partly overlap with it resulting in the (v_{Al}-O_N) center ionization and an electron transfer into the conduction band. This assumption is confirmed experimentally by considerable large energy accumulation in the crystalline lattice of AlN observed under its irradiation with 245 nm light, which can be released either optically as OSL or thermally as TL [3-10]. Further the electron from the conduction band can be captured by one of numerous electron traps (levels from 7 up to 11) which form a number of donor levels situated below the conduction band [37, 38]. The O_N defect – a close neighbor of the ionized (v_{Al}-O_N) is one of them (level 7) and after an electron capture it is transformed into the $(O_N)^-$ center. In the same time after an electron loss the (v_{Al}-O_N) center is transformed into the $(v_{Al}$-$O_N)^+$ center containing a trapped hole. Recombination of the $(v_{Al}$-$O_N)^+$ and $(O_N)^-$ centers with emission of a light quantum (hv_{lum}) results in the UV-blue luminescence.

Really, it is highly possible that before formation of the $(O_N)^-$ center the electron from the conduction band can be repeatedly captured and released from other different electron traps, which are located in a close vicinity of the main defect (levels 8 to 11). This assumption is confirmed by experimentally observed time-dependent gradual rise of the UV-blue luminescence under continuous excitation until saturation (Fig. 3 A).

According to the energy level scheme shown in Fig. 12 the similar recombination luminescence process can occur when AlN is irradiated with light quanta from the fundamental absorption edge generating an electron/hole pair (hv_{fund}) or exciton (hv_{ex}). In this case the energy transfer from the host material to the oxygen-related defects takes place resulting in the $(v_{Al}$-$O_N)^+$ and $(O_N)^-$ center formation and UV-blue light emission. As it is seen from the PLE spectra (Fig. 2, curve 1), which demonstrates luminescence yield under different excitations, the host lattice excitation around 200 nm (band-to-band transitions or exciton creation) with the following energy transfer to the oxygen-related defects is more

efficient for formation of the UV-blue luminescence than the direct excitation of these defects within their absorption band at 245 nm.

As mentioned above it is known that the position of maximum of the UV-blue PL band varies within the spectral range 350 nm - 420 nm for AlN ceramics samples of different origin [27-29] and this variation highly depends on concentration of the oxygen-related defects in the material. Youngman and Harris [27] showed that the maximum of the UV-blue luminescence linearly varies from 350 nm up to 380 nm when the oxygen concentration increases from 0,3 up to 0,75 atomic percents in AlN ceramics. In our measurements a position of this band reaches even 420 nm (Fig. 5) confirming that the oxygen concentration exceeds a value of 0,75 atomic percents in this sample. The observed behavior – dependence of the UV-blue PL band's position on oxygen concentration shown in the Fig. 5 could be explained by change of close environment of luminescence centers.

4.1.2 480 nm luminescence

The 480 nm band appears in complex PL spectra of AlN ceramics overlapping with the UV-blue PL band discussed above. For AlN ceramics this PL band is well pronounced only in the case of 200 nm excitation corresponding to band-to-band or exciton transitions (Fig. 1, curve 1). This PL is also characterized with its own defect-induced excitation (absorption) forming a band at 285 nm (Fig. 2, curve 2) which is different but in the same time partly overlapping with the 245 nm band responsible for UV-blue PL excitation. In the case of the AlN ceramics the UV-blue PL around 400 nm is always predominant over the 480 nm band which usually appears as asymmetric shoulder of complex spectrum (see Fig. 1). Otherwise it is in the case of AlN powder – a raw material for AlN ceramics. The 480 nm PL becomes predominant not only in the case of its direct excitation at 285 nm but even under the 242 nm corresponding to the UV-blue PL excitation while intensity of the UV-blue PL is low (Fig. 7). This phenomenon is more pronounced in the case of nano-structured AlN powder where the 480 nm PL is also predominant but the UV-blue PL is hardly detectable even under its own excitation at 245 nm (Fig. 8).

The present knowledge level about the features of 480 nm luminescence of AlN, unfortunately, does not allow reveal the defects involved in the luminescence process and construct their energy level scheme as it has been done for the UV-blue luminescence. Nevertheless, the 480 nm PL features mentioned above directly demonstrate that decrease of AlN material size (from ceramics to powder and further to nano-powder) results in increase of the relative intensity of the 480 nm band compared to that of the UV-blue PL band. It means that in this row of materials with decreasing size the contribution of the luminescence centers responsible for the 480 nm PL increases and in the case of nano-structured material it takes even over those responsible for the UV-blue luminescence. In the same time it is known that reduction of the size of material results in considerable enlargement of its surface area. This phenomenon allows the conclusion that the surface defects could be directly responsible for the 480 nm PL of AlN.

The spectral characteristics discussed above of both the 480 nm and UV-blue PL seem to be similar. These considerations allow the proposal that the 480 nm PL in AlN could be also caused by some sort of the oxygen-related defects, which are located at or near the surface of the material in the same time having possible more complicated structure in comparison with those producing the UV-blue luminescence.

4.1.3 600 nm luminescence

The third PL band around 600 nm (the red PL band) is always observed in the complex spectra of bulk AlN (Fig.1). This PL band can be excited either at 200 nm corresponding to the band-to-band or exciton transitions or within their own defect-related excitation bands at 260 nm and 400 nm (Fig. 6, curve 1), which differ from those observed for the UV-blue and

480 nm PL excitation (Fig. 2). However the 260 nm band overlaps with the 245 nm band of the UV-blue PL excitation (Fig. 6, curves 1 and 2). The 400 nm excitation band of the red PL largely overlaps with the UV-blue emission resulting in its re-absorption and transformation into the red luminescence.

It seems that there are different luminescence centers responsible for the red PL and the UV-blue PL. From Fig. 5 it is seen that the ratio of intensities of the red PL and other part of the spectrum consisting of the UV-blue and 480 nm bands alters from sample to sample of different origin. Moreover, our previous investigations showed that the red luminescence of AlN ceramics appears in both the TL spectra and the spectra of luminescence afterglow observed when luminescence excitation is ceased [29, 31].

All of these features mentioned above allow conclusion that the red PL of AlN is also caused by the recombination process. Like the case of the UV-blue PL it is very probable that the red PL characterizes the bulk AlN. However, the red PL is also observed in the case of AlN nanotips and nanorods [13, 32, 33] but is not observed in AlN nano-powder (Fig. 8). Nevertheless, it seems that there is not any contradiction because as it was mentioned above the dimension of the nanotip only at its top reaches ~10 nm but at the base it exceeds 100 nm. It means that only the top of nanotip is true nanomaterial whereas the whole volume of the tip could be considered rather as a bulk material.

For a long time the defects responsible for the red PL in AlN were unknown. In the paper of Sarua et al this luminescence is attributed to the processes involving defects formed from nitrogen vacancies (v_N) and excess Al (see Ref.39 and references therein).

4.2 PL features at material size reduction from bulk to nanoscale

The present investigation of PL in AlN macro size materials (ceramics and powder) as well as in nanostructured materials (nanopowder, nanotips and nanorods) shows that the same three PL bands are observed in all of these materials within the spectral range from 250 nm up to 700 nm and no other new band appears (Figs. 1, 7, 8, and 9), however the ratio of intensities of these bands highly depends on material structure and origin as well as on excitation way.

This investigation is focused on the UV-visible PL consisting of both the UV-blue luminescence around 400 nm and 480 nm band. Several peculiarities of this luminescence can be derived from the results above depending on material size.

One of the main characteristics observed can be related to the decrease of the PL intensity when material size is reduced. This feature is demonstrated in Fig. 9 where the PL spectra are shown for the bulk AlN (ceramics), nanorods and nanotips (curves 1, 2 and 3, correspondingly). These spectra are measured under the same experimental conditions and are converted to one and the same constant number of exciting light quanta at 200 nm, therefore demonstrating the relative luminescence yield for these different samples. This PL feature is also observed for AlN powder and nanosize powder.

In the same time the positions of maxima of UV-blue PL band are shifted to higher energies (shorter wavelengths) when material size is reduced from bulk AlN (ceramics) to nanorods and nanotips as it is shown in Fig. 10. These two phenomena could be explained by diminution of concentration of oxygen-related defects in material range above when its size is reduced from macro- to nano-scale.

The mechanisms of UV-visible luminescence excitation also depend on material size. As it is seen from the excitation spectra demonstrated in Figs. 2 and 11 and energy level scheme in Fig. 12, there are two channels of the UV-blue PL excitation. One of them is caused by energy transfer from the host lattice excitation (electron/hole pairs or excitons) to the oxygen-related defects with proceeding PL, whereas another is related to the direct excitation of an oxygen-related defect by light from its own absorption band. In the case of the bulk AlN (ceramics) it is seen that intensity of the UV-blue PL at 200 nm excitation is twice as large as that caused by the direct excitation of oxygen-related defect at 245 nm (Fig. 2, curve 1) and

the first cannel of excitation is more efficient than the second one. In the case of AlN nanorods (and also AlN nanotips) the first excitation cannel is even more pronounced. For nanomaterials the main way of defect excitation is realized through energy transfer from the host crystalline lattice (see Fig. 11). The observed phenomenon could be explained by presence of lower concentration of the oxygen-related defects in the nanostructured materials compared to that of the bulk material. Direct defect excitation refers only to the defects situated in the near-surface layer depending on a penetration depth of absorbed light and defect concentration is low. Whereas in the case of excitation of the host material the energy transfer can reach the defects situated within the whole volume of the material.

In summary, the results above demonstrating the influence of material size on features of the UV-blue PL allow conclusion that the same luminescence centers caused by the oxygen-related defects are active in both the bulk AlN (ceramics and powder) and nanostructured materials (AlN nanorods, nanotips and nanopowder). The main difference of luminescence properties is the following. In the case of the nanostructured materials the concentration of native oxygen-related defects is smaller than that observed for the bulk AlN materials and the energy transfer from the excited host material to defects is the main excitation channel. The 480 nm PL band which could be ascribed to surface defects appears in AlN ceramics, powder and nanopowder. In the case of AlN nanorods and nanotips this band is hardly pronounced.

5 CONCLUSIONS

1. The present investigation shows that besides the well known PL bands around 400 nm and 600 nm the 480 nm luminescence also appears in different structures of AlN such as ceramics, macrosize powder and nanostructured materials – nanorods and nanopowder. The 480 nm luminescence preferably can be excited by light quanta from fundamental absorption band resulting in creation of the electron/hole pairs or excitons, although there is its own defect-induced excitation/absorption band at 285 nm. The ratio of the intensities of 400 nm and 480 nm PL bands highly depends on the material structure as well as excitation energy; nevertheless, the 480 nm PL band usually appears as asymmetric long wavelength shoulder in the complex UV-blue luminescence spectra. The defects responsible for the 480 nm luminescence are yet unknown. Nevertheless, similarity of spectral characteristics of both the 400 nm and 480 nm PL allows assumption that in luminescence processes forming the last band some kind of the oxygen-related defects is also involved. A role of the surface defects on formation of this luminescence is discussed.
2. According to the literature data and results of the present investigation the energy level scheme of defects responsible for the UV-blue PL at 400 nm is constructed revealing the mechanism and recombination character of this luminescence.
3. It was found that within the spectral range from 250 nm up to 700 nm the same PL bands at 400 nm, 480 nm and 600 nm are observed and no other new PL band appears when a size of material is reduced from bulk (AlN ceramics, macrosized powder) to nanoscale (nanopowder, nanorods, nanotips), nevertheless, a ratio of the intensities of these bands highly depends on material size and excitation way. In the same time, reduction of material size results in decrease of luminescence intensity of the main UV-blue band. In the case of the nanostructured materials – nanorods and nanotips the energy transfer from the host material to the defects responsible for luminescence is the main channel for the defect excitation considerably prevailing over the defect direct excitation. This phenomenon could be explained by the assumption that in the bulk AlN material concentration of the oxygen-related defects prevails over that observed for nanostructured materials.

Acknowledgments

The present investigation was supported by Grant of Latvian Scientific Council Nr 05.1722 and Grant from European Community Nr VPD1/ERAF/CFLA/05/APK/2.5.1./000064/031.

References

[1] A. Kobayashi, O. F. Sankey, S. M. Volz, and J. D. Dow, "Semiempirical tight-binding band structures of wurtzite semiconductors: AlN, CdS, CdSe, ZnS, and ZnO," *Phys. Rev. B* **28***,* 935-945 (1983) [doi:10.1103/PhysRevB.28.93].

[2] N. E. Christensen and I. Gorczyca, "Optical and structural properties of III-V nitrides under pressure," *Phys. Rev. B* **50**, 4397-4415 (1994) [doi:10.1103/PhysRevB.50.4397].

[3] L. Trinkler, P. Christensen, N. A. Larsen, and B. Berzina, "Thermoluminescence properties of AlN ceramics," *Rad. Meas.* **29**, 341-348 (1998) [doi:10.1016/S1350-4487(98)00007-9].

[4] L. Trinkler, A. J. J. Bos, A. J. M. Winkelman, P. Christensen, N. A. Larsen, and B. Berzina, "Thermally and optically stimulated luminescence of AlN ceramics," *Rad. Prot. Dosim*. **84**, 207-210 (1999).

[5] L. Trinkler, L. Botter-Jensen, P. Christensen, and B. Berzina, "Studies of AlN ceramics for application in UV dosimetry," *Rad. Prot. Dosim*. **92**, 299-306 (2000).

[6] L. Trinkler, L. Botter-Jensen, P. Christensen, and B. Berzina, "Stimulated luminescence of AlN ceramics by ultraviolet radiation," *Rad. Meas.* **33**, 731-735 (2001) [doi:10.1016/S1350-4487(01)00093-2].

[7] L. Trinkler, L. Boetter-Jensen, and B. Berzina, "Aluminum nitride ceramics: a potential UV dosimeter material," *Rad. Prot. Dosim* **100**, 313-316 (2002).

[8] L. Trinkler, B. Berzina, and M. Benabdelesselam, "Use of AlN ceramics in ultraviolet radiation dosimetry," *Proc. SPIE* **5123**, 49-54 (2003) [doi: 10.1117/12.517003].

[9] L. Trinkler, B. Berzina, A. Auzina, M. Benabdesselam, and P. Iacconi, "UV light energy storage and thermoluminescence in AlN ceramics," *phys. stat. sol. (c)* **4**, 1032-1035 (2007).

[10] L. Trinkler, B. Berzina, A. Auzina, M. Benabdesselam, and P. Iacconi, "Use of aluminium nitride for UV radiation dosimetry," *Nucl. Instrum. Meth. A* **580**, 354-357 (2007) [doi:10.1016/j.nima.2007.05.177].

[11] E. Silveira, J. A. Freitas, G. A. Slack, L. J. Schowalter, M. Kneissl, D. W. Treat, and N. M. Johnson, "Depth-resolved cathodoluminescence of a homoepitaxial AlN thin film," *J. Cryst. Growth* **281,** 188-193 (2005) [doi:10.1016/j.jcrysgro.2005.03.024].

[12] G. M. Prinz, A. Ladenburger, M. Feneberg, M. Schirra, S. B. Thapa, M. Bickermann, B. M. Epelbaum, F. Scholz, K. Thonke, R. Sauer, "Photoluminescence, cathodoluminescence and reflectance study of AlN Layers and AlN single crystals," *Superlatt. Microstruct.* **40,** 513-518 (2006) [doi:10.1016/j.spmi.2006.10.001].

[13] S. C. Shi, C. F. Chen, S. Chattopadhyay, K. H. Chen, B. W. Ke, L. C. Chen, L. Trinkler, and B. Berzina , "Luminescence properties of wurtzite AlN nanotips," *Appl. Phys. Lett.* **89,** 163127-1(2006) [doi:10.1063/1.2364158].

[14] B. Berzina, L. Trinkle, J. Grabis, and I. Steins, "Photoluminescence in AlN: macro-size and nanopowder," *phys. stat. sol.* (c) **4**, 959-962 (2007).

[15] C. Balasubramanian, V. P. Godbole, A. K. Das, V. K. Rohatgi, and S. V. Bhoraskar, "Synthesis of nanowires and nanoparticles of cubic aluminium nitride," *Nanotechnol.* **15,** 370-373 (2004) [doi: 10.1088/0957-4484/15/3/024].

[16] C. Balasubramanian, S. Bellucci, P. Castrucci, M. De Crescenzi, S. V. Bhoraskar, "Scanning tunneling microscopy observation of coiled aluminum nitride nanotubes," *Chem. Phys. Lett.* **383,** 188-191 (2004) [doi: 10.1016/j.cplett.2003.11.028].

[17] S. Bellucci, "Carbon nanotubes and semiconducting nanostructures: current views and future perspectives," *CANEUS 2004-Conf. Micro-Nano-Technologies*, AIAA 6752, Monterey, CA (Nov. 2004).

[18] S. Bellucci, C. Balasubramanian, G. Cinque, A. Marcelli, M. Cestelli Guidi, M. Piccinini, A. Popov, A. Soldatov, P. Onorato, "Characterization of aluminum nitride nanostructures by XANES and FTIR spectroscopies with synchrotron," *Coatings, Adhesives and Composites*, Nanotech. vol. 1, Chap. 3., pp. 233 – 238, NSTI, Cambridge, MA (2006).

[19] C. Balasubramanian, S. Bellucci, G. Cinque, A. Marcelli, M. Cestelli Guidi, M. Piccinini, A. Popov, A. Soldatov, and P. Onorato, "Characterization of aluminium nitride nanostructures by XAFNES and FTIR spectroscopies with synchrotron radiation," *J. Phys.: Condens. Matter* **18** S2095-S2104 (2006) [doi: 10.1088/0953-8984/18/33/S25].

[20] S. Bellucci, C. Balasubramanian, A. Ivanov, A. Popov, and H. Schober, "Neutron characterization of aluminium nitride nanotubes," *J. Neutron Res*. **14,** 287-291 (2006) [doi: 10.1080/10238160601049054].

[21] Yu. F. Zhukovskii, A. I. Popov, C. Balasubramanian, and S. Bellucci, "Structural and electronic properties of single-walled AlN nanotubes of different chiralities and sizes," *J. Phys.: Condens. Matter* **18,** S2045– S2054 (2006) [doi:10.1088/0953-8984/18/33/S20].

[22] Yu. F. Zhukovskii, N. Pugno, A. I. Popov, C. Balasubramanian, and S. Bellucci, "Influence of *F* centers on structural and electronic properties of AlN single-walled nanotubes," *J. Phys.: Condens. Matter* **19,** 395021 (2007) [doi:10.1088/0953-8984/19/39/395021].

[23] S.-C. Shi, S. Chattopadhyay, C.-F. Chen, K.-H. Chen, and L.-C. Chen, "Structural evolution of AlN nano-structures: nanotips and nanorods," *Chem. Phys. Lett.* **418,** 152-157 (2006) [doi:10.1016/j.cplett.2005.10.107].

[24] G. A. Slack, "Nonmetalic crystals with high thermal conductivity," *J. Phys. Chem. Solids* **34** 321-335 (1973) [doi:10.1016/0022-3697(73)90092-9].

[25] G. A. Slack and T. F. McNelly, "Growth of high purity AlN crystals," *J. Cryst. Growth* **34,** 263-279 (1976) [doi:10.1016/0022-0248(76)90139-1].

[26] G. A. Slack, R. A. Tanzilli, R. O. Pohl, and J. W. Vandersande, "The intrinsic thermal conductivity of AIN," *J. Phys. Chem. Solids* **48**, 641-647 (1987) [doi:10.1016/0022-3697(87)90153-3].

[27] R. A. Youngman and J. H. Harris, "Luminescence studies of oxygen-related defects in aluminum nitride," *J. Am. Ceram. Soc*. **73,** 3238-3246 (1990) [doi:10.1111/j.1151-2916.1990.tb06444.x].

[28] J. H. Harris, R. A. Youngmann, and R. G. Teller, "On the nature of the oxygen-related defects in aluminum nitride," *J. Mater. Res.* **5,** 1763-1773 (1990) [doi:10.1557/JMR.1990.1763].

[29] E. Palcevskis, B. Berzina, L. Trinkler, U. Ulmanis, and N. Mironova-Ulmane, "Ceramics from fine plasma processed AlN powder, sintering and properties," *Latvian J. Phys. Technol. Sci*. **1**, 34-52 (1999).

[30] B. Berzina, L. Trinkler, J. Sils, and E. Palcevskis, "Oxygen-related defects and energy accumulation in aluminum nitride ceramics," *Rad. Eff. Def. Solid.* **156**, 241-247 (2001) [doi:10.1080/10420150108216900].

[31] B. Berzina, L. Trinkler, J. Sils, and K. Atobe, "Luminescence mechanisms of oxygen-related defectsin AlN," *Rad. Eff. Def. Solid.* **157**, 1089-1092 (2002) [doi:10.1080/10420150215822].

[32] L. Trinkler, B. Berzina, L. C. Shi, M. Benabdesselam, and P. Iacconi, "UV light induced luminescence processes in AlN nanotips and ceramics," *phys. stat. sol. (c)* 2 1, 334-338 (2005).

[33] L. Trinkler, B. Berzina, D. Kasjan, and L.-Ch. Chen, "Luminescence processes induced by UV radiation in AlN nanotips and nanorods," *Rad. Meas.* **43,** 231-235 (2008) [doi:10.1016/j.radmeas.2007.12.025].

[34] S. Bellucci, A. I. Popov, C. Balasubramanian, G. Cinque, A. Marcelli, I. Karbovnyk, V. Savchyn, and N. Krutyak, "Luminescence, vibrational and XANES studies of AlN nanomaterials," *Rad. Meas.* **42,** 708-711 (2007) [10.1016/j.radmeas.200701.072].

[35] J. Grabis, "Nanosized nitrate-based composite powders produced by ICP technique," *Interface Controlled Materials*, M. Ruehle and M. Gleitzer, Eds., pp. 267-272, Wiley-VCG, Weinheim, Germany (2000) [doi:10.1002/352760622X.ch43].

[36] S. Shwiezer, U. Rogulis, J. M. Spaeth, L. Trinkler, and B. Berzina, "Investigation of oxygen-related luminescence centers in AlN ceramics," *phys. stat. sol. (b)* **219,** 171-180 (2000).

[37] T. L. Tansley and R. J. Egam, "Point defect energies in the nitrides of aluminum, gallium, and indium," *Phys. Rev.* **B 45,** 10942-10950 (1992) [doi:10.1103/PhysRevB.45.10942].

[38] D. W. Jenkins and J. D. Dow, "Electronic structure and dopping of InN, In_xGa_{x-1} N, and $In_xAl_{x-1}N$," *Phys. Rev.* **B 39, 5** 3317-3329 (1989).

[39] A. Sarua, S. Rajasingam, M. Kuball, N. Garro, O. Sancho, A. Cros, A. Cantarero, D. Olguin, B. Liu, D. Zhuang, and Edgar, "Effect of impurities on Raman and photoluminescence spectra of AlN bulk crystals," *Proc. Mater. Res. Soc. Symp.* **708,** Y5.17 (2003).